Pergamon

Bioorganic & Medicinal Chemistry, Vol. 4, No. 10, pp 1605–1615, 1996

PII: S0968-0896(96)00152-6
0968-0896/96 $15.00+0.00

Synthesis and Biochemical Activity of Novel Amidine Derivatives as m1 Muscarinic Receptor Agonists

Babatunde Ojo,[†] Philip G. Dunbar,[‡] Graham J. Durant,[§] Peter I. Nagy, James J. Huzl, III, Sumudra Periyasamy, Dan O. Ngur, Afif A. El-Assadi, Wayne P. Hoss and William S. Messer, Jr*

Department of Medicinal and Biological Chemistry, Center for Drug Design and Development, College of Pharmacy, The University of Toledo, 2801 West Bancroft Street, Toledo, OH 43606, U.S.A.

Abstract—As part of a continuing effort aimed at the development of selective, efficacious, and centrally active m1 muscarinic agonists for the treatment of Alzheimer's disease, a series of amide and hydrazide amidine derivatives (**2a–e** and **3b–d**) was synthesized and examined for muscarinic agonist activity. Preliminary biochemical studies indicated that **2b**, **2d**, and **3d** bound to muscarinic receptors in rat brain and stimulated phosphoinositide (PI) metabolism in rat cerebral cortex. Compounds **2b** and **2d** were also highly efficacious at m1 muscarinic receptors expressed in cultured A9 L cells. Molecular modeling studies suggest slightly different modes of interaction with m1 receptors for the ester and amide derivatives. Also, hydrogen-bond formation with a Thr residue may be important for m1 muscarinic agonist potency. The data suggest that the amide moiety can replace the ester group found in muscarinic agonists and provide further support for the utility of amidine derivatives in the development of efficacious m1 agonists. Copyright © 1996 Elsevier Science Ltd

Introduction

Muscarinic m1 receptors are distributed predominately in the mammalian forebrain (cerebral cortex and hippocampus), located mainly on postsynaptic neurons and their relative density appears to be unaltered in Alzheimer's disease.[1] Furthermore, a preferential involvement of muscarinic m1 receptors in memory and other cognitive functions has been tentatively proposed, whereas activation of central and peripheral muscarinic m2 and m3 receptors appears more closely linked with the production of undesirable side effects.[2,3]

The past decade has witnessed considerable research efforts focused on the development of muscarinic agonists. One of the principal reasons for this is the therapeutic potential of a centrally active muscarinic agonist in Alzheimer's disease.[4] Nonselective muscarinic agonists such as arecoline and RS 86 have been extensively studied in Alzheimer's disease patients; but results have been very discouraging due to the high incidence of cholinergic side effects.[5,6]

Collectively, these and other data suggest that selective cholinergic agonists acting directly on muscarinic receptors in the central nervous system (CNS) may be useful in the therapeutic management of Alzheimer's disease by improving the defective cholinergic function associated with the disease. Based on the activity of compound **1b**, which was a selective and highly efficacious m1 muscarinic agonist,[7] our chemical efforts continued with the evaluation of a series of tetrahydropyrimidine oxadiazole derivatives.[8]

In an effort to improve this activity, as well as to determine the structure–activity parameters of this class of compounds as m1 muscarinic receptor agonists, our synthetic endeavour focused on the design of analogues of **1b** and **1e** (the only compounds in series **1** considered here), which embodied replacement of the metabolically labile ester moiety. In the studies outlined here we have investigated the use of amide and hydrazide functionalities as potential isosteric replacements for the ester group contained in **1b**. Computer modeling allowed us to examine, at the molecular level, possible differences in the binding mode of ligands to muscarinic receptors. The data presented here describe the synthesis and biological evaluation of a series of novel muscarinic agonists which may serve as lead compounds for the development of selective m1 agonists.

Results

Synthetic chemistry

A series of amide and hydrazide ester bioisosteres were synthesized via amidation and hydrazinolysis of the corresponding reduced pyrimidine-5-carboxylic acid

[†]Present address: Department of Medicinal Chemistry, School of Pharmacy, Medical College of Virginia, Virginia Commonwealth University, Richmond, VA 23298, U.S.A.
[‡]Present address: Washington State University, Health Research and Education Center, Spokane, WA 99204, U.S.A.
[§]Present address: Cambridge Neuroscience, Inc., One Kendall Square, Building 700, Cambridge, MA 02139, U.S.A.
Key words: muscarinic receptors, amidine derivatives, selectivity, M_1 agonists, molecular modeling.

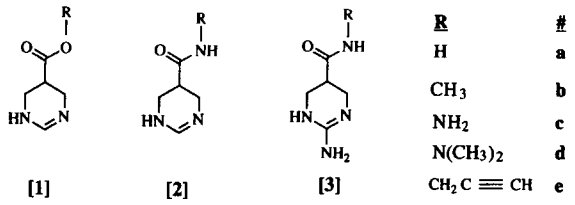

Chemical structures. Not all combinations were synthesized and tested.

and 2-aminopyrimidine-5-carboxylic acid derivatives (see Schemes 1 and 2). A halogen–metal exchange reaction,[9] utilizing *n*-butyl lithium at −100 °C followed by carboxylation with dry ice was employed to prepare pyrimidine-5-carboxylic acid from the commercially available 5-bromopyrimidine. The acid then was reduced[10] readily in aq acid over 10% Pd–C to form the 1,4,5,6-tetrahydropyrimidine-5-carboxylic acid.

2-Aminopyrimidine-5-carboxylic acid was synthesized using literature procedures.[11] The acid was catalytically reduced using the same method as indicated above to form 2-amino-1,4,5,6-tetrahydropyrimidine-5-carboxylic acid. For producing amides, in each series the reduced acids were first converted to their acid chloride derivatives using an oxalyl chloride solution in benzene followed by an amidation reaction with the desired amine (e.g. ammonia, *N*-methylamine, and propargylamine) to yield the corresponding 1,4,5,6-tetrahydropyrimidine-5-carboxamides (**2a–b**, **2e**, and **3b**). In the case of the hydrazides, the reduced acids were first converted to their methyl ester derivatives by heating at reflux in methanol with thionyl chloride as the dehydrating agent. Hydrazinolysis reaction of the methyl ester derivatives in methanol gave the corresponding hydrazides (**2c–d** and **3c–d**).

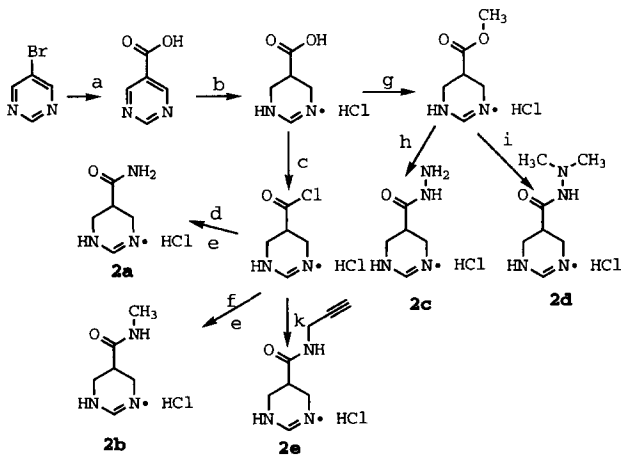

Scheme 1. Reaction conditions: (a) *n*-BuLi, CO_2; (b) H_2, Pd-on-carbon (10%), aq HCl; (c) oxalyl chloride solution in benzene, reflux; (d) NH_3, CH_2Cl_2, triethylamine; (e) ethereal HCl (1 M); (f) methylamine, CH_2Cl_2, DBU; (g) $SOCl_2$, MeOH, reflux; (h) hydrazine, methanol, reflux; (i) *N,N*-dimethylhydrazine, methanol, reflux; (k) propargylamine, CH_2Cl_2, triethylamine.

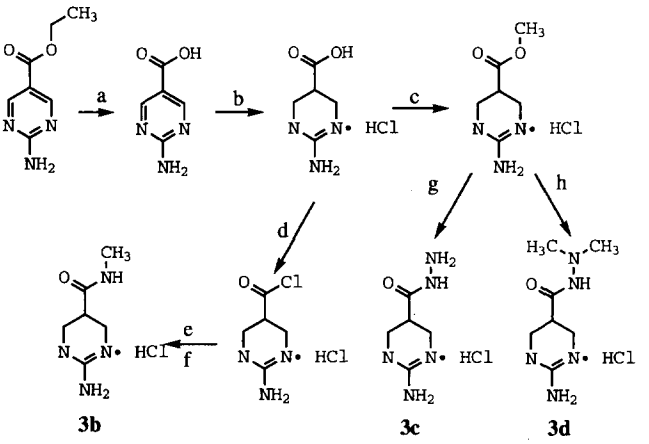

Scheme 2. Reaction conditions: (a) KOH, methanol, reflux; (b) H_2, Pd-on-carbon (10%), aq HCl; (c) $SOCl_2$, MeOH, reflux; (d) oxalyl chloride solution in benzene, reflux; (e) methylamine, CH_2Cl_2, DBU; (f) ethereal HCl (1 M); (g) hydrazine, methanol, reflux; (h) *N,N*-dimethylhydrazine, methanol, reflux.

Computational Chemistry

Relative energies and (absolute) molecular volumes were compared for the protonated conformers of **1b**, **1e**, **2b**, **2d**, **2e**, **3b**, **3d**, and **3e** as shown in Table 1. Structures within a 5 kcal/mol relative energy range were obtained by energy minimization using the AMBER force field (see Experimental) on a set of conformers found in a multiconformational search upon rigid rotations.

In each of the series, the tetrahydropyrimidine ring exhibited a similar position relative to the side-chain. There were two low-energy conformations found for each methyl amide derivative (**2b** and **3b**). There were four low-energy conformations for each hydrazide (**2d** and **3d**), while five and six low-energy conformations were found for each propargylic amide analogue (**2e** and **3e**), respectively. The data for **1b** and **1d** have been reported previously.[12] The 1,4,5,6-tetrahydropyrimidine methyl ester (**1b**) was the smallest in terms of molecular volume followed closely by its corresponding *N*-methylamide analogue (**2b**). Molecular volumes were largest for **3d** with the bulky amine group. The nearly constant difference of the molecular volumes of 10–12 Å^3 for **2b–3b**, **2d–3d**, and **2e–3e** indicates additive volume contributions due to the 2-NH_2 in series **3**. It suggests no unfavored steric interaction between the 2-amino group and the 5-substituent.

The results of superimposition studies of conformers **1b**, **2b**, **2d**, **3b**, and **3d** are shown in Table 2. Small RMS values indicate conformations that can be superimposed closely (e.g. **1b** i and **3b** ii), however, the energy ranks of the matching conformers do not correspond necessarily. Similar observations were made for the propargyl analogues (e.g. **1e** i and **2e** v in Tables 1 and 3).

Docking studies on **1b**, **2b**, and **2d** were performed using a recently developed nine-amino acid model of

the binding site of the muscarinic m1 receptor.[13] The binding energy (BE) was determined from the total energy of the ligand/receptor complex minus the individual energies of the ligand and receptor model.

Table 1. Relative energies and molecular volumes for several amidine derivatives

	Compound	Relative energies (kcal/mol)	Molecular volume (Å^3)
1b	i	—	131.5
	ii	2.0	129.4
	iii	2.5	130.2
1e	i	—	153.2
	ii	1.8	153.2
	iii	1.9	154.1
2b	i	—	134.5
	ii	2.8	135.0
2d	i	—	163.5
	ii	3.2	163.6
	iii	4.4	162.7
	iv	4.7	163.7
2e	i	—	156.8
	ii	0.03	157.0
	iii	0.04	157.0
	iv	0.9	157.4
	v	2.7	157.5
3b	i	—	146.2
	ii	3.4	145.4
3d	i	—	174.6
	ii	0.1	173.9
	iii	0.3	173.9
	iv	2.6	175.1
3e	i	—	167.7
	ii	0.1	168.7
	iii	0.4	168.0
	iv	0.9	168.4
	v	1.3	168.4
	vi	4.6	167.7

Data for **1b** and **1e** have been reported previously.[12]

Computer modeling of **1b**, **2b**, and **2d** interacting with the m1 receptor binding site indicated electrostatic interactions and hydrogen bonds between the protonated amidine moiety and the carboxylate of Asp105 in almost all dimer structures (see Table 4). However, different binding modes were found for the 5-substituents in series **1** and **2**. The ether oxygen accepted a hydrogen bond from the hydroxyl group of Thr192 [see Figure 1(a)] for **1b** with a BE of −19.73 kcal/mol (Table 4). This interaction is impossible with the amides and hydrazides where the NH group in place of the ether oxygen has proton donor characteristics. Accordingly, dimers with ligands in series **2** are stabilized in another way: the methyl groups in **2b** and **2d** can favorably interact with nonpolar side chains [see Figures 1(b) and 1(c)]. Contributions to the binding energy of **2b** and **2d** show that the van der Waals terms are more negative by about 4 kcal/mol than those for **1b**, resulting in considerably more negative BE values for **2b** and **2d** than for **1b**.

Calculations for the propargyl derivatives (**1e** and **2e**) revealed that **1e** has a BE of −25.2 kcal/mol in its most stable binding mode. The docked structure, starting from a ligand conformation when the propargyl group is rotated toward Asn382, was higher in energy by about 0.3 kcal/mol. The position of **2e** in its more stable binding mode is close to that of **1e** (BE = −25.7 kcal/mol). The binding mode for **2e** with the rotated propargyl group was higher in energy however, by about 1.5 kcal/mol. A large portion (1.1 kcal/mol) of this energy increase comes from the increase of the ligand internal energy. The molecular mechanics rotational potential curve for **2e** shows considerable increase (mainly due to increase of the van der Waals energy) upon increasing the H—N—C—C torsional angle from its minimum position of 0°. A torsional angle of about 40°, found in the optimized dimer upon ligand binding, is in line with the internal energy increase of 1.1 kcal/mol.

Table 2. Superimposition rms values (in Å with two significant digits) for a series of amidine derivatives

		1b			**2b**		**3b**		**2d**				**3d**			
		i	ii	iii	i	ii	i	ii	i	ii	iii	iv	i	ii	iii	iv
1b	i	—	1.0	1.0	1.2	*0.07*	1.2	*0.07*	1.2	1.2	0.55	1.3	1.3	1.3	1.2	0.55
	ii		—	0.76	0.39	1.0	0.42	1.0	0.39	0.37	1.2	0.57	0.572	0.94	0.413	1.2
	iii			—	0.41	1.0	0.39	1.0	0.41	0.43	1.2	0.923	0.94	0.569	0.38	1.2
2b	i				—	1.2	*0.04*	1.2	*0.04*	*0.05*	1.4	0.67	0.68	0.70	*0.06*	1.4
	ii					—	1.2	*0.03*	1.2	1.2	0.56	1.3	1.3	1.3	1.2	0.56
3b	i						—	1.2	*0.06*	*0.08*	1.4	0.67	0.70	0.68	*0.05*	1.4
	ii							—	1.2	1.2	0.56	1.3	1.3	1.3	1.2	0.58
2d	i								—	0.33	1.7	0.77	0.78	1.3	*0.04*	1.7
	ii									—	1.6	0.923	0.93	1.0	0.334	1.6
	iii										—	1.6	1.3	1.3	1.7	*0.03*
	iv											—	*0.03*	1.2	1.5	1.7
3d	i												—	0.76	0.808	1.7
	ii													—	0.788	1.6
	iii														—	1.7
	iv															—

Small values are italicized and indicate a close match of corresponding atoms in the different compounds.

Table 3. Superimposition rms values (in Å with two significant digits) for a series of amidine derivatives

		1e			**2e**					**3e**					
		i	ii	iii	i	ii	iii	iv	v	i	ii	iii	iv	v	vi
1e	i	—	1.2	1.2	1.5	1.3	1.3	0.61	*0.07*	0.59	0.59	1.5	1.3	1.3	*0.07*
	ii		—	0.98	0.53	1.1	0.51	1.0	1.2	1.5	1.0	0.50	1.0	0.51	1.2
	iii			—	0.50	0.51	1.0	1.5	1.3	1.0	1.6	0.53	0.51	1.1	1.2
2e	i				—	0.68	0.69	1.4	1.5	1.4	1.4	*0.04*	0.67	0.70	1.5
	ii					—	1.2	1.4	1.3	1.1	1.4	0.70	*0.04*	1.2	1.3
	iii						—	1.2	1.3	1.4	1.2	0.66	1.2	*0.04*	1.3
	iv							—	0.62	1.1	*0.03*	1.4	1.4	1.1	0.62
	v								—	0.61	0.60	1.5	1.3	1.3	*0.03*
3e	i									—	1.1	1.4	1.2	1.4	0.61
	ii										—	1.4	1.4	1.1	0.60
	iii											—	0.68	0.68	1.5
	iv												—	1.2	1.3
	v													—	1.3
	vi														—

Small values are italicized and indicate a close match of corresponding atoms in the different compounds.

Biological data

The receptor binding affinity of each compound was determined indirectly by assessing the inhibition of specific ^{3}H-(R)-QNB binding to rat brain membranes. The *N*-methylamide, 1,4,5,6-tetrahydropyrimidine-5-carboxylic-*N*-methylamide hydrochloride (**2b**), displayed approximately tenfold lower affinity ($IC_{50}=90$ μM) than the methyl ester (**1b**). Compound **2d** displayed a moderate affinity ($IC_{50}=32$ μM) for muscarinic receptors in the rat central nervous system. The *N,N*-dimethylhydrazide, 2-amino-1,4,5,6-tetrahydropyrimidine-5-carboxylic-*N,N*-dimethylhydrazide hydrochloride (**3d**), displayed an intermediate affinity ($IC_{50}=99$ μM). The unsubstituted amides and hydrazides in each series were inactive ($IC_{50}>100$ μM) in binding assays (see Table 5).

The compounds with reasonable affinity (IC_{50} values <100 μM) also were evaluated for their ability to stimulate phosphoinositide (PI) metabolism in the rat cerebral cortex at a single concentration. The *N*-methylamide, 1,4,5,6-tetrahydropyrimidine-5-carboxylic-*N*-methylamide hydrochloride (**2b**), displayed moderate agonist activity, stimulating PI turnover to 110% above basal levels at 100 μM. In contrast, the propargyl amide (**2e**) exhibited no detectable agonist activity. Compound **2d** displayed higher activity (270%

Table 4. Binding energies for the docking of differet conformers of ligands **1b**, **2b**, and **2d** to the 9-amino acid model of the m1 muscarinic receptor

	Ligand conformer	Binding energy (kcal/mol)	Relative binding energy (kcal/mol)	Hydrogen bond Asp105 (Å)	Hydrogen bond Thr192 (Å)	Hydrogen bond Asn382 (Å)
1b	i	−19.73	0	1.83	2.06	—
1b	iii	−17.78	1.95	1.94 2.57	—	—
1b	ii	−17.23	2.50	1.72	2.72	—
1b	i	−16.49	3.24	—	2.17	—
2b	i	−25.01	0	1.87	—	—
2b	i	−23.60	1.40	1.87 2.77	2.66	—
2b	i	−22.62	2.38	1.96	—	—
2b	iii	−22.44	2.56	2.13 2.78	2.61	—
2b	iii	−20.32	4.69	—	2.74	2.41
2d	iii	−26.45	0	2.81 2.71	2.89	—
2d	iv	−25.15	1.30	2.94	2.69	—
2d	i	−24.61	1.84	2.95 2.94	2.23	—
2d	iii	−23.25	3.20	2.70 2.78	—	—
2d	ii	−22.96	3.32	—	2.44	—

Bond distances (for potential hydrogen bonds) within 3.00 Å are shown for the three residues believed to beinvolved in the binding of muscarinic agonists to m1 receptors.

stimulation above basal levels at 100 μM) at muscarinic receptors coupled to PI metabolism in the rat cerebral cortex. The *N,N*-dimethylhydrazide, 2-amino-1,4,5,6-tetrahydropyrimidine-5-carboxylic-*N,N*-dimethylhydrazide hydrochloride (**3d**), displayed much lower activity, stimulating PI turnover to only 59% above basal levels at 100 μM.

Based on their activity in the cerebral cortex, the potencies and efficacies of compounds **2b** and **2d** were determined at m1 muscarinic receptors expressed in A9 L cells (see Table 6). Compound **2b** was found to be efficacious (~60% of carbachol response) at m1 muscarinic receptors, although **2b** was approximately four times less potent than **1b** and 20-fold less potent

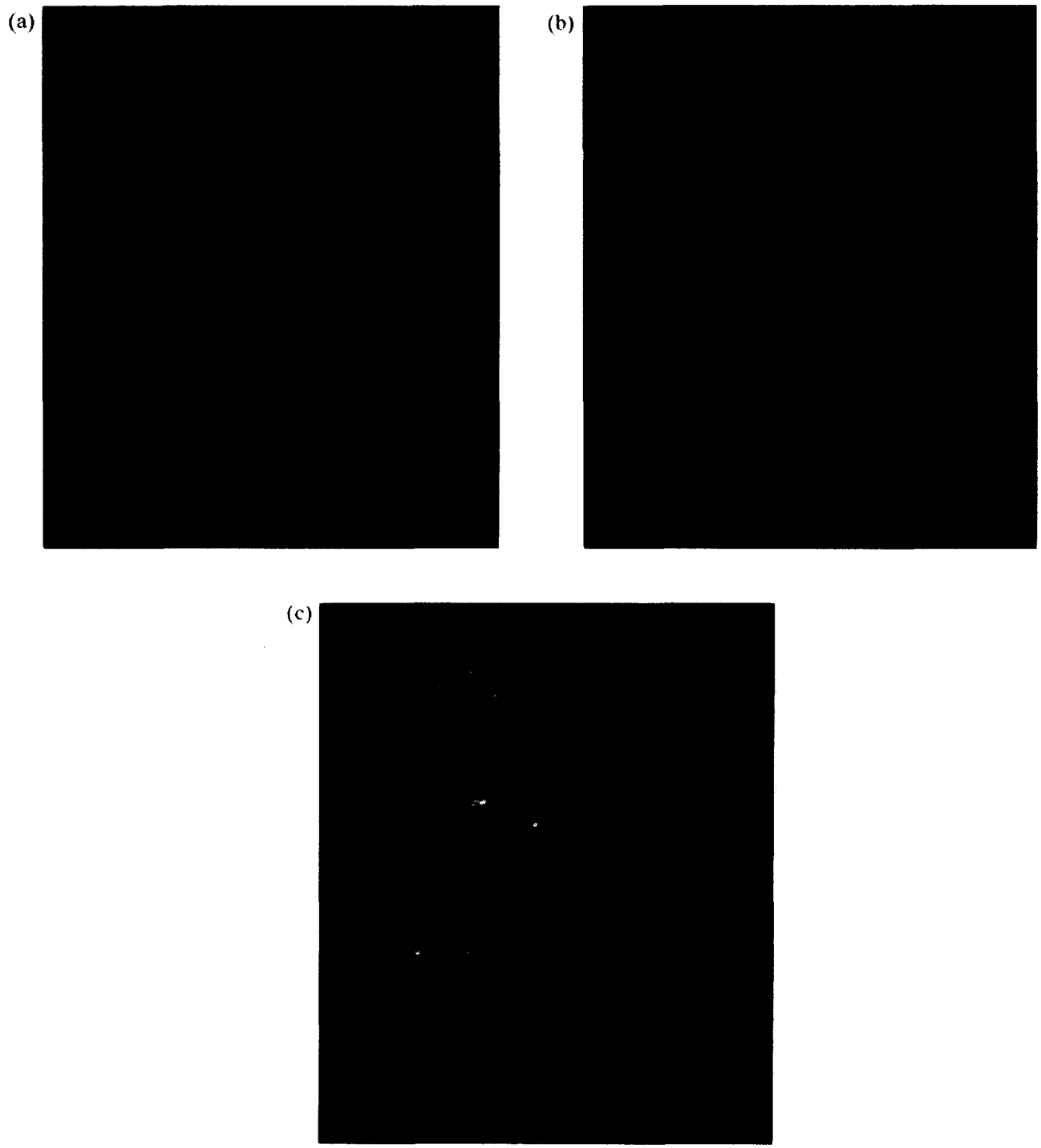

Figure 1. Docking of ligands into a model of the m1 muscarinic receptor binding site (recently developed by Nordvall and Hacksell[13]). Six of the nine amino acids are depicted in yellow, while Asp105, Thr192 and Asn381 are colored by atom type (C = white; H = light blue; O = red; N = dark blue). The ligand also is colored by atom type. (a) Docking of conformation i of **1b** into a model of the m1 muscarinic receptor binding site. Hydrogen bonds (within 2.1 Å) are indicated by dashes between Asp105 and the amidine group and between Thr192 and the ether oxygen. (b) Docking of conformation i of **2b** into a model of the m1 muscarinic receptor binding site. Hydrogen bonds (within 2.1 Å) are indicated by dashes between Asp105 and the amidine group. (c) Docking of conformation i of **2d** into a model of the m1 muscarinic receptor binding site.

Table 5. The inhibition of ^{3}H-(R)-QNB binding to rat brain membranes by amidine derivatives

Ligand	IC_{50} values (μM)	PI at 100 μM (%)
Carbachol	5.5±1.0	470±81
Arecoline	1.0±0.25	110±21
1b	9.2±1.9	110±11
1e	3.3±0.80	230±35
2a	>100	n.d.
2b	90±79	110±10
2c	>100	n.d.
2d	32±17	270±55
2e	7.5±2.7	0.7±0.9
3b	>100	n.d.
3c	>100	n.d.
3d	99±26	59±8.7

Also shown is the stimulation of PI metabolism in rat cortical slices. Data represent the mean (±SEM) from three assays each performed in triplicate. Phosphoinositide activity was not determined (n.d.) for ligands with IC_{50} values >100 μM. Previously published data for carbachol, arecoline, **1b** and **1e** are presented here for comparison.[7]

Table 6. Potency and efficacy in a series of amidine-containing ligands at m1 muscarinic receptors expressed in A9 L cells

Ligand	EC_{50} (μM)	S_{max} (%)
Carbachol	40±15	630±110
1b	200±51	660±110
2b	760±320	380±61
2d	300±120	410±68

Data represent the mean (SEM) from three experiments, each performed in triplicate. Data for carbachol and **1b** were presented previously in preliminary fashion.[33]

than carbachol. Similarly, compound **2d** displayed high efficacy (~65% of carbachol response), yet low potency at m1 muscarinic receptors.

Discussion

The data described above clearly demonstrate that amides and hydrazides are useful as ester isosteres, and may provide structural leads for the design of more efficacious muscarinic agonists. Such ligands should have improved oral bioavailability relative to muscarinic agonists containing ester groups, such as arecoline. Although, the amide and hydrazide derivatives are less potent than the lead ester (**1b**), they are remarkably efficacious and warrant further development as m1 agonists. It is important to note that only the secondary amides displayed muscarinic receptor binding and activity. Primary amides (e.g. **2a**) and tertiary amides (data not shown) were inactive at muscarinic receptors in rat brain.

The low potencies of **2b** and **2d** at m1 receptors suggest an important role for the hydrogen bond acceptor site in agonist potency, rather than efficacy (Table 6). This is consistent with previous findings based on ligand considerations,[14-18] which have indicated the presence of two hydrogen bonding interactions as a necessary requirement for binding with high affinity to the agonist binding site of the receptor. The low potency of the guanidine derivatives could be due to the presence of the amino group which might force the substituents at position 5 further away from Asp105, resulting in improper alignment of the ester group for hydrogen-bonding interactions with important residues at the binding site. The relative contributions of the amide and guanidine groups in activation of muscarinic receptors can be determined through site-directed mutagenesis studies of muscarinic receptor subtypes, a goal for future work.

A previous study with other muscarinic agonists, as exemplified by pilocarpine, indicate that the carbonyl oxygen is of primary importance for agonist activity while the ether oxygen is of secondary or lesser importance.[19] In the studies outlined here, the superimposition of **1b** upon **2b** and **2d** [see Figures 2(a) and 2(b)] revealed that the carbonyl oxygen functionality assumed nearly the same position in space, *suggesting* that these ligands may be interacting with muscarinic receptors in a similar fashion.

In the docking studies, the rings of ligands were set nearly in the same positions relative to the receptor in the starting orientations. For **1b** i, a long-range electrostatic attraction was found to favor the formation of a hydrogen bond between the ether oxygen and Thr192. The gradient optimization method in the docking procedure moved the ligand in this direction without consideration of the depth of the energy minimum to be reached. Without such dominating electrostatic effects as in the case of **2b**, where N—H cannot favorably form a hydrogen bond to Thr192, van der Waals attraction may be comparable with electrostatic forces and move the ligand toward another binding mode. The large number of methyl groups in the nonpolar side chains of the receptor model favors the binding modes for **2b** and **2d** as shown in Figures 1(b) and 1(c).

The BE for **1b** is less negative than found for **2b**, despite having the methyl groups occupy nearly the same position in some conformers (e.g. see rms values of **1b** i and **2b** ii, Table 2). This is in contrast to the higher potency found for compound **1b**. In fact, when replacing **2b** (in its most favorable orientation relative to the receptor) by **1b** and starting a new docking procedure from this position, optimization for the **1b**–receptor dimer yielded a structure with a BE of −23,93 kcal/mol. This means that even the **1b** structure can be much more strongly bound in another mode than in Figure 1(a) (though the optimized ligand is moved slightly toward the Thr192 hydroxyl group, due to the possibilty for a favorable hydrogen bond with the ether oxygen). Furthermore, Table 4 indicates several hydrogen bonds to Thr192 for the **2** series of ligands, where the lone pairs of the amide and hydrazide Ns act as H acceptors or there are hydrogen bonds to the carbonyl oxygens. (In these latter cases,

however, the methyl groups of the ligands move away from the nonpolar side chains of the receptor resulting in less negative BE.) In total, van der Waals interactions and hydrogen bonds produce BEs more negative for **2b** and **2d** than for the identified modes with **1b**.

Potency and efficacy are, however, considerably more favorable for **1b** than for **2b** or **2d**, as shown in Table 6. The inverse relationship between activity and BE can be resolved assuming that the most negative binding modes for compounds **2** do not represent the biologically relevant binding mode for acting as an agonist. If a nonbiologically relevant mode is of the most negative BE, the chance for binding and triggering the required agonist activity is reduced.

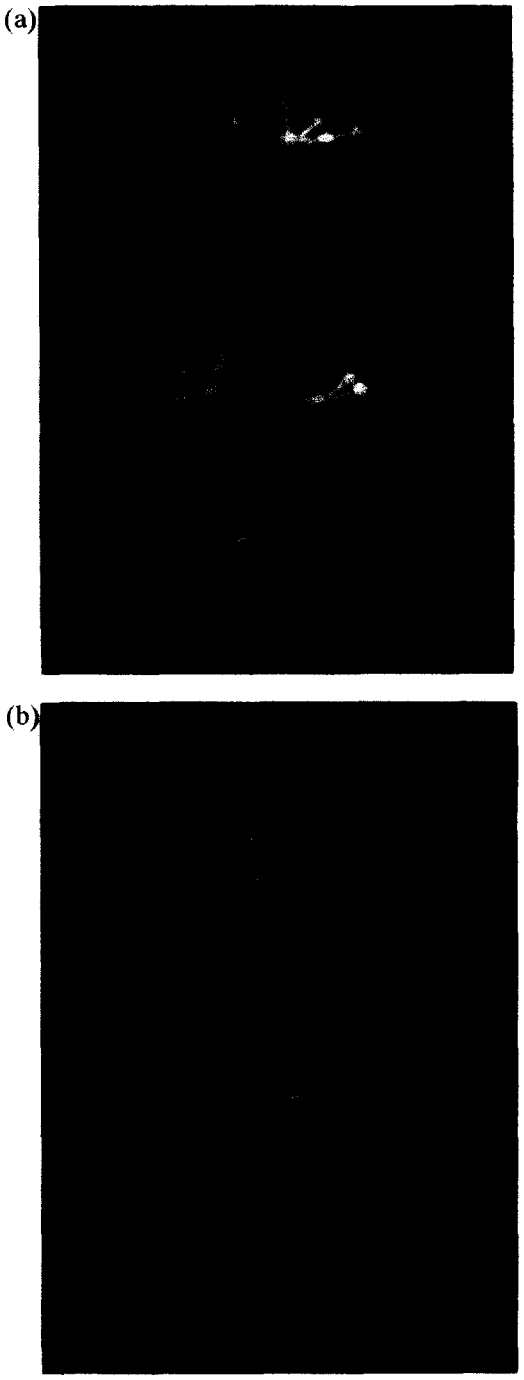

Figure 2. (a) Superimposition of conformation i of **1b** with conformation ii of **2b**. (b) Superimposition of conformation i of **1b** with comformation iii of **2d**.

Modeling may provide some rationale for the agonist and antagonist characteristics of **1e** and **2e**, respectively (Table 5). Both ligands, with BE more negative than −25 kcal/mol, have the most stable binding mode without hydrogen bonding to Thr192, which is in contrast to **1b**. For **1e** and **2e** the strong binding comes through van der Waals interactions of the propargyl group with the receptor. From a biological point-of-view, however, it seems to be important whether the propargyl group points toward the Asn382 side chain. The optimized BE for the structure when propargyl points closer to Asn is higher in energy only by 0.3 kcal/mol for **1e**, but by 1.5 kcal/mol for **2e**. Thus, a change in the binding mode for **2e** requires considerably higher energy than for **1e**. The antagonist character of **2e** may be related to this larger energy requirement for reaching the binding mode with the propargyl group moved toward Asn382.

In summary, we believe that high potency for an m1 agonist can be reached if there are short hydrogen bonds of about 2 Å with both Asp105 and Thr192 at the same time or an extended substituent group can readily point toward Asn382 while maintaining the hydrogen bond to Asp105. Experimentally highly potent agonists (**1b** and **1e**) met one or the other binding mode based on computer modeling. Conformational changes for **2e** require too much energy for reaching an arrangement supposedly required for an agonist with extended group. Indeed, our preliminary mutagenesis experiments with m3 receptors indicate a smaller importance of the Asn side chain for agonists with *small* R substituents.

The significance of the data reported here is that small changes in structure lead to dramatic changes in the binding mode of agonists. Despite the more negative binding energy, the binding modes for compounds **2b** and **2d** were quite different from the modes of interaction for more potent and efficacious ligands. These data suggest that the binding mode is predominately responsible for agonist activity. It must be kept in mind, however, that conclusions about the agonist potency are based on a simple comparison of the BE values and potentially very important contributions due to entropic and solvent effects have been neglected.

In future studies, the effect of further structural modifications will be examined, with particular emphasis on the functional selectivity of these and other amidine derivatives at other muscarinic receptor subtypes. Eventually, such compounds might be therapeutically useful in the treatment of the cognitive impairments and memory deficits associated with Alzheimer's disease.

Experimental

Chemistry

Compounds were synthesized utilizing reagent grade chemicals commercially available from Aldrich Chemical Co. and Fisher Scientific without further purification. NMR spectra were obtained on a Bruker ACF 300 MHz NMR in deuterochloroform, deuteromethanol or deuterium oxide, using TMS as an internal standard. MS were recorded on a Hewlett Packard 5890 spectrometer. TLC was perfomed on Kodak Chromatogram sheet 13181 silica gel with a fluorescent indicator (F254). Melting points were taken on an Electrothermal digital melting point apparatus and are presented uncorrected. Elemental analyses were performed by M-H-W Laboratories, Phoenix, Arizona, and were within $\pm 0.4\%$ of theoretical values.

1,4,5,6-Tetrahydropyrimidine-5-carboxylic amide HCl (2a). 1,4,5,6-Tetrahydropyrimidine-5-carboxylic acid hydrochloride[7] (0.4 g, 2.1 mmol) was suspended in a solution of oxalyl chloride (0.4 mL, 4.3 mmol) in benzene (10 mL), heated with stirring under reflux for 2.5 h, and then evaporated to dryness in vacuo after cooling, to give an orange–yellow residue. The last traces of oxalyl chloride were removed by adding 10 mL of benzene to the residue, then the residue was evaporated in vacuo to give an orange residue of the crude acid chloride. It should be noted that benzene was utilized due to its solvent properties for the conversion of the acid to the acid chloride. Also, excess oxalyl chloride was removed more easily with benzene than with toluene, which normally would be used due to its comparatively low toxicity.

The residue was suspended in dry dichloromethane (30 mL) containing DBU (1,8-diazabicyclo[5.4.0]undec-7-ene) 98% (0.6 mL, 4.3 mmol) under a nitrogen atmosphere and cooled to 0 °C. The solution was allowed to warm to room temperature, and then saturated with excess gaseous ammonia until the solution was basic. The solids, a mixture of product and ammonium chloride, were filtered off. The mixture was taken up in water (40 mL), extracted (6×150 mL) with dichloromethane and the extracts were dried ($MgSO_4$). The extracts were combined and evaporated to dryness in vacuo to give a residue of the free base. The hydrochloride salt was obtained by addition of 1 M HCl in ether to an ethanol solution of the residue, evaporation of solvents to dryness in vacuo and recrystallization (ethanol/ether) to give pale-yellow crystals (0.2 g, 61%) of 1,4,5,6-tetrahydropyrimidine-5-carboxylic amide as the hydrochloride salt: mp 165–167 °C; ^{1}H NMR (CD_3OD): δ 3.0 (m, 1H), 3.5 (d, 4H), 5.82–6.04 (br s, 2H, NH_2), 7.9 (s, 1H); MS: *m/z* 127 (M^+ of free base). Anal. calcd ($C_5H_{10}N_3OCl$): C, 32.71; H, 6.16; N, 20.68. Found: C, 32.11; H, 6.45; N, 20.53% (carbon off 0.6% in elemental analysis).

1,4,5,6-Tetrahydropyrimidine-5-carboxylic-*N*-methylamide HCl (2b). 1,4,5,6-Tetrahydropyrimidine-5-carboxylic acid hydrochloride[7] (0.5 g, 3.1 mmol) was converted to the acid chloride and then reacted with methylamine hydrochloride in the presence of DBU employing a method virtually identical to that used for **2a**. The crude product was recrystallized from ethanol:diethyl ether to yield crystals (0.7 g, 62%) of 1,4,5,6-tetrahydropyrimidine-5-carboxylic-*N*-methylamide as the hydrochloride salt: mp 150–151 °C; ^{1}H NMR (D_2O): δ 2.4 (d, 3H), 2.80 (q, 1H), 3.09 (m, 1H), 3.5 (d, 4H), 7.8 (s, 1H). Anal. calcd ($C_6H_{12}N_3OCl$): C, 40.57; H, 6.81; N, 23.66. Found: C, 40.69; H, 6.85; N, 23.70%.

1,4,5,6-Tetrahydropyrimidine-5-carboxylic hydrazide HCl (2c). 1,4,5,6-Tetrahydropyrimidine-5-carboxylic acid hydrochloride[7] (1.1 g, 6.2 mmol) was dissolved in anhyd methanol (50 mL), and thionyl chloride (0.3 mL, 1.4 mmol) was added dropwise with stirring at room temperature. The solution was refluxed overnight for 24 h and then evaporated to dryness in vacuo. The resulting crude residue was recrystallized from methanol:diethyl ether to give white crystals (1.1 g, 96%) of the methyl ester. The methyl ester,[7] dissolved in hydrazine monohydrate 98% (0.8 mL, 16.6 mmol), was refluxed in methanol (20 mL) for 2 h, and then evaporated to dryness in vacuo to give a pink residue. Recrystallization of the residue from methanol and diethyl ether gave crystals (0.3 g, 49%) of 1,4,5,6-tetrahydropyrimidine-5-carboxylic hydrazide as the hydrochloride salt: ^{1}H NMR (CD_3OD): δ 2.7 (m, 1H), 3.0 (m, 1H), 3.5 (d, 4H), 5.85–6.04 (br d, 2H, NH_2), 7.9 (s, 1H); MS: *m/z* 142 (M^+ of free base). Anal. calcd ($C_5H_{11}N_4OCl$): C, 33.62; H, 6.21; N, 31.37. Found: C, 33.50; H, 6.07; N, 31.59%.

1,4,5,6-Tetrahydropyrimidine-5-carboxylic-(*N*,*N*-dimethyl)hydrazide HCl (2d). 5-(Methyloxycarbonyl)-1,4,5,6-tetrahydropyrimidine hydrochloride[7] (0.5 g, 2.8 mmol) and *N*,*N*-dimethylhydrazine 98% (1.0 mL, 13.2 mmol) were refluxed in anhyd methanol (20 mL) for 2 h, and then evaporated to dryness in vacuo to give a yellow residue. Recrystallization of the residue from absolute ethanol and diethyl ether yielded crystals (0.3 g, 51%) of 1,4,5,6-tetrahydropyrimidine-5-carboxylic-(*N*,*N*-dimethyl)hydrazide as the hydrochloride salt: mp 180–181 °C; ^{1}H NMR (D_2O): δ 2.8 (s, 1H), 3.1 (m, 1H), 3.5 (d, 4H), 3.7 (s, 6H), 7.8 (s, 1H); MS: *m/z* 180 (M^+ of free base). Anal. calcd ($C_7H_{15}N_4OCl$): C, 40.68; H, 7.32; N, 27.11. Found: C, 40.71; H, 7.30; N, 27.23%.

Propargyl-1,4,5,6-tetrahydropyrimidine-5-carboxamide HCl (2e). 1,4,5,6-Tetrahydropyrimidine-5-carboxylic acid hydrochloride[7] (1.3 g, 7.9 mmol) was converted to the acid chloride and then reacted with propargylamine in the presence of DBU by a method virtually identical to that used for **2a**. The crude product was recrystallized from ethanol:diethyl ether to yield brown crystals (0.5 g, 58%) of propargyl-1,4,5,6-tetrahydropyrimidine-5-carboxamide as the hydrochloride salt: mp 169–170 °C; ^{1}H NMR (D_2O): δ 1.4 (q, 1H), 2.1 (q, 1H, acetylenic-H), 3.09 (m, 1H), 3.5 (d, 4H), 3.6 (t, 2H, $HCCCH_2$), 7.8 (s, 1H, amidine-H). Anal. calcd ($C_8H_{12}N_3OCl$): C, 47.65; H, 6.00; N, 20.84. Found: C, 47.81; H, 6.05; N, 20.75%.

2-Amino-1, 4, 5, 6-tetrahydropyrimidine- 5 -carboxylic-*N*-methylamide HCl (3b). 2-Amino-1,4,5,6-tetrahydropyrimidine-5-carboxylic acid hydrochloride[12] (0.3 g, 1.7 mmol) was converted to the acid chloride and then reacted with methylamine hydrochloride in the presence of DBU employing a method virtually identical to that used for **2a**. The crude product was recrystallized from ethanol:diethyl ether to yield crystals (0.5 g, 59%) of 2-amino-1,4,5,6-tetrahydropyrimidine-5-carboxylic-*N*-methylamide as the hydrochloride salt: mp 154–155 °C; ^{1}H NMR (D_2O): δ 2.4 (d, 3H), 2.9 (q, 1H), 3.1 (m, 1H), 3.5 (d, 4H). Anal. calcd ($C_6H_{13}N_4OCl$): C, 37.41; H, 6.80; N, 29.09. Found; C, 37.55; H, 6.87; N, 29.15.

2-Amino-1,4,5,6-tetrahydropyrimidine-5-carboxylic hydrazide HCl (3c). 2-Amino-5-(ethyloxycarbonyl)pyrimidine[11] (0.1 g, 0.7 mmol) was reduced catalytically over palladium-on-carbon 10% (0.1 g, 0.9 mmol) in aq HCl at room temperature for 4 h. Hydrogenation was carried out on a Parr apparatus at 29 psi to give a white residue of 2-amino-5-(ethyloxycarbonyl)-1,4,5,6-tetrahydropyrimidine. The reduced ester was then reacted with hydrazine monohydrate 98% (0.3 mL, 6.2 mmol) by a method virtually identical to that used for **2c**. Recrystallization of the crude residue from methanol:diethyl ether yielded crystals (80.4 mg, 67%) of 2-amino-1,4,5,6-tetrahydropyrimidine-5-carboxylic hydrazide as the hydrochloride salt: mp 125–126 °C; ^{1}H NMR (D_2O): δ 2.7 (m, 1H, geminal coupling; 15 Hz), 3.09 (m, 1H), 3.5 (d, 4H), 5.82–6.04 (br d, 2H, NH_2); MS: *m/z* 156 (M^+ of free base). Anal. calcd ($C_5H_{12}N_5OCl$): C, 31.01; H, 6.25; N, 36.17. Found: C, 31.20; H, 6.22; N, 36.19%.

2-Amino-1,4,5,6-tetrahydropyrimidine-5-carboxylic-(*N*,-*N*-dimethyl) hydrazide HCl (3d). 2-Amino-1,4,5,6-tetrahydropyrimidine-5-carboxylic acid[8] (0.1 g, 0.5 mmol) was esterified in anhyd methanol by a method virtually identical to that used for **2c**. The resulting methyl ester then was reacted with *N*,*N*-dimethylhydrazine 98% (0.4 mL, 5.3 mmol) employing a method similar to that used for **2d**. The crude product was recrystallized from from ethanol:diethyl ether to yield crystals (40 mg, 58%) of 2-amino-1,4,5,6-tetrahydropyrimidine-5-carboxylic-(*N*,*N*-dimethyl)hydrazide as the hydrochloride salt: mp 192–193 °C; ^{1}H NMR (D_2O): δ 2.8 (s, 1H), 3.0 (m, 1H), 3.50 (d, 4H), 3.65 (s, 6H); MS: *m/z* 156 (M^+ of free base). Anal. calcd ($C_7H_{16}N_5OCl$): C, 37.92; H, 7.28; N, 31.59. Found: C, 37.97; H, 7.30; N, 31.62%.

Computational chemistry

Molecular modeling on the isolated ligand molecules was described in detail previously.[12] The main steps were as follows: generation of structures was performed using MacroModel 4.5[20] on an Indigo2 SGI worksation. MNDO electrostatic potential (ESP) fitted charges[21] were obtained using MOPAC 6.0[22] running on a DEC Alpha 3000/500. Energies of structures were minimized using the AMBER all atom force field[23] (as implemented in MacroModel) and ESP-fitted charges described above. Conformational searching in the torsional space was performed using the multiconformer method[24] applying rigid rotation in 30° increments when rotating the ester, amide, or hydrazide plane relative to the tetrahydropyrimidine ring and the freely rotatable exocyclic substituents. Conformers with energy above the minimum by no more than 5 kcal/mol were saved for full geometry optimization. Obtained structures were submitted to single point MOPAC calculations to generate a new set of ESP fitted atomic charges. New charges were imported into the MacroModel file and the energy minimization was repeated. Molecular mechanics optimization and update of the ESP charges were repeated as long as the charges and the geometries reached convergence.

In docking studies, the m1 receptor was modeled by a nine-amino acid residue structure proposed recently.[13] Where necessary, NH_2 and C(O)—CH_3 end-groups were added to the residue backbones cut out from a protein structure. A negatively charged side chain was assumed for Asp105. Atomic charges, both for the residues in the model and the protonated ligands to be docked, were obtained from AM1 calculations which describe hydrogen-bonded systems adequately.[25]

Docking was performed using the DOCK procedure of the Sybyl 6.1 modeling package[26] that utilizes the Tripos force-field and user-defined charges. The procedure minimizes the interaction energy of the receptor model (site) and the ligand by changing their relative positions. Throughout the docking, geometry changes for the ligand were allowed while the structure of the site was kept fixed, in order to avoid the collapse of the residues in portions of space not filled by the ligand. Since the calculated binding energy BE = E(dimer) − E(ligand) − E(receptor) refers to a specific binding mode, not necessarily corresponding either to the minimum energy arrangement or the biologically relevant ligand–receptor structure, several modes have been explored. Taking local energy minimum conformations for the ligands (Table 1) different starting orientations of the ligand relative to the site were defined. Placing the cationic head of the ligand at a distance of 2–3 Å from the Asp105 carboxylate group, the ligand was rotated about the C5-C(side chain) bond in increments of 90°. Occasionally emerging close contacts with the site atoms were removed by translating the ligand by about 1 Å still maintaining the alignment of the charged groups. Separate dockings from the different starting orientations were performed resulting in binding energies and hydrogen-bond patterns as shown in Table 4.

Gas-phase modeling has been supported by considering the possible hydration of the ligand–receptor model dimer. Using the precomputed box procedure of Sybyl, no water molecules were found between the receptor and ligand in the binding pocket after hydration. Water was found nearby, however, e.g. in the neighborhood of the negatively charged Asp105 residue. These water molecules could stabilize the ion-pair interaction

assumed in the present modeling, based on experimental findings.

For comparison of the binding modes of **1e** and **2e** with agonist and antagonist character, respectively, two sets of calculations were initiated. Docking for **1e** was conducted as described above. Docking studies for **2e** started with the ligand arrangement superimposed to the optimal **1e** position. In the second pair of calculations, the propargyl group was rotated by about 120° in order to approach the amide group of Asn382. For reasons mentioned earlier, the receptor model was kept as a fixed site.

Receptor binding

Receptor binding studies were carried out in an indirect fashion by evaluating the ability of ligands to compete with 50 pM ^{3}H-(R)-quinuclidinyl benzilate (^{3}H-(R)-QNB) in a suspension of brain membranes, as previously described.[27] Nonspecific binding was evaluated by the inclusion of 1000-fold excess atropine in a separate set of samples, and the IC_{50} values were subsequently determined from Hill plots of the inhibition data. The values are here reported as means ±SEM of three independent experiments each performed in triplicate.

Phosphoinositide metabolism

Phosphoinositide metabolism studies were performed utilizing a slight modification of the method of Brown and associates,[28] as previously described.[29,30] The cerebral cortex was dissected according to the method of Glowinski and Iversen. [31] The inositol, ^{3}H inositol, used in these studies was first purified by passing over a Dowex AG1-X8 anion exchange column to remove charged degradation products of ^{3}H inositol, and then used for the assays. The amount of ^{3}H inositol phosphates formed in the assay was determined utilizing a slight modification of the method of Wreggett and Irvine,[32] in which case the separation of inositol phosphates was accomplished using an Amersham Super Separator Manifold.

Biochemical assays in cultured cell lines

The compounds were evaluated for muscarinic agonist activity in cultured A9 L cells expressing m1 muscarinic receptor subtypes to assess their potencies and efficacies. A9 L cells used in these studies were kept as monolayer cultures in a 175 cm^2 polystyrene tissue culture flasks at 37 °C, aerated with 95% O_2 and 5% CO_2. Cell viability was evaluated through direct microscopic examination (10 × magnification). Cells from the tissue culture flask were carefully transferred into 20 mL of cold growth medium maintained at a temperature of 4 °C, and then collected by high speed (1600 × *g*, 4500 rpm in a J2-21/E Beckman centrifuge) centrifugation for 5 min at 4 °C. The cells were subsequently suspended in 1.5 mL of a freezing medium (10% DMSO), and kept tightly capped in a 2 mL plastic freezing tube. Each tube was kept frozen and stored under a nitrogen atmosphere at −20 °C for 2 h.

Intact A9 L cells expressing m1 muscarinic receptors were incubated with ^{3}H *myo*-inositol (0.5 μCi/well) in 24-well plates (plating density of 10^5 cells per well) in 0.5 mL of DMEM, aerated with 95% O_2 and 5% CO_2 for 48 h. After 48 h incubation, the medium was aerated and the cells were washed twice with a 1 mL DMEM containing 10 mM LiCl. The medium was replaced by 0.45 mL of the same medium (10 mM LiCl), and then incubated for an additional 20 min at 37 °C. The reaction sequence was initiated by the addition of 50 μL of the appropriate agonist concentrations (or medium), and allowed to proceed for an additional 0.5 h. After the incubation period, the reaction was quenced by aeration of the medium followed by addition of 0.5 mL of a 5% (v/v) ice-cold trichloroacetic acid (TCA). The wells were washed with 0.5 mL of distilled water, and then added to the TCA extract. The TCA extract was placed on top of a Dowex-Formate columns (Biorad AG1-X8 resin, formate form, 100–200 mesh), and washed three times with 3 mL of 5 mM of *myo*-inositol. Total ^{3}H inositol phosphates were then eluted with 1 mL of 0.1 M ammonium formate/0.1 formic acid. After the elution, 0.5 mL of the eluate was counted in 10 mL of Cytoscint on a TM Analytic beta counter.

Acknowledgments

This work was supported by grants NS 01493, NS 31173, and the Ohio Department of Aging. The authors also would like to acknowledge the synthetic chemical efforts of Rita Lodoya.

References

1. Araujo, D. M.; Lapchak, P. A.; Robitaille, Y.; Gauthier, S.; Quirion, R. *J. Neurochem.* **1988**, *50*, 1914.

2. Messer, Jr W. S.; Bohnett, M.; Stibbe, J. *Neurosci. Lett.* **1990**, *116*, 184.

3. Chermat, R.; Simon, P.; Boissier, J. R. *J. Pharmacol.* **1976**, *7*, 227.

4. Moos, W.; Davis, R. E.; Schwarz, R. D.; Gamzu, E. R. *Med. Res. Rev.* **1988**, *8*, 353.

5. Christie, J. E.; Shering, A.; Ferguson, J.; Glen, A. I. M. *Br. J. Psychiat.* **1981**, *138*, 46.

6. Bruno, G.; Mohr, E.; Gillespie, M.; Fedio, P.; Chase, T. N. *Arch. Neurol.* **1986**, *43*, 659.

7. Messer, Jr W. S.; Dunbar, P. G.; Rho, T.; Periyasamy, S.; Ngur, D.; Ellerbrock, B. R.; Bohnett, M.; Ryan, K.; Durant, G. J.; Hoss, W. *Bioorg. Med. Chem. Lett.* **1992**, *2*, 781.

8. Dunbar, P. G.; Durant, G. J.; Fang, Z.; Rho, T.; Abuh, Y. F.; El-Assadi, A. A.; Ngur, D.; Periyasamy, S.; Hoss, W.; Messer, Jr W. S. *J. Med. Chem.* **1993**, *36*, 842.

9. Gronowitz, S.; Roe, J. *Acta Chem. Scand.* **1965**, *19*, 1741.

10. Smith, V. H.; Christensen, B. E. *J. Org. Chem.* **1955**, *20*, 829.

11. Schenone, P.; Sansebastino, L.; Mosti, L. *J. Heterocycl. Chem.* **1990**, *27*, 295.

12. Dunbar, P. G.; Durant, G. J.; Rho, T.; Ojo, B.; Huzl, III J. J.; Smith, D. A.; El-Assadi, A. A.; Sbeih, S.; Ngur, D. O.; Periyasamy, S.; Hoss, W.; Messer, Jr W. S. *J. Med. Chem.* **1994**, *37*, 2774.

13. Nordvall, G.; Hacksell, U. *J. Med. Chem.* **1993**, *36*, 967.

14. Freedman, S. B.; Patel, S.; Harley, E. A.; Iversen, L. L.; Baker, R.; Showell, G. A.; Saunders, J.; McKnight, A.; Newberry, N.; Scholey, K.; Hargreaves, R. *Eur. J. Pharmacol.* **1992**, *215*, 135.

15. Saunders, J.; Cassidy, M.; Freedman, S. B.; Harley, E. A.; Iversen, L. L.; Kneen, C.; MacLeod, A. M.; Merchant, K. J.; Snow, R. J.; Baker, R. *J. Med. Chem.* **1990**, *33*, 1128.

16. Street, L. J.; Baker, R.; Book, T.; Kneen, C. O.; MacLeod, A. M.; Merchant, K. J.; Showell, G. A.; Saunders, J.; Herbert, R. H.; Freedman, S. B.; Harley, E. A. *J. Med. Chem.* **1990**, *33*, 2690.

17. Ngur, D.; Rocknich, S.; Messer, Jr W. S.; Hoss, W. *Biochem. Biophys. Res. Comm.* **1992**, *187*, 1389.

18. Ward, J. S.; Merritt, L.; Klimkowski, V. J.; Lamb, M. L.; Mitch, C. H.; Bymaster, F. P.; Sawyer, B. D.; Shannon, H. E.; Olesen, P. H.; Honoré, T.; Sheardown, M. J.; Sauerberg, P. *J. Med. Chem.* **1992**, *35*, 4011.

19. Shapiro, G.; Floersheim, P.; Boelsterli, J.; Amstutz, R.; Bolliger, G.; Gammenthaler, H.; Gmelin, G.; Supavilai, P.; Walkinshaw, M. *J. Med. Chem.* **1992**, *35*, 15.

20. Mohamadi, F.; Richards, N. G. J.; Guida, W. C.; Liskamp, R.; Lipton, M.; Caufield, C.; Chang, G.; Hendrickson, T.; Still, W. C. *J. Comput. Chem.* **1990**, *11*, 440.

21. Singh, U. C.; Kollman, P. A. *J. Comput. Chem.* **1984**, *5*, 129.

22. Stuart, J. J. P. In QCPE no. 455: Bloomington, Indianna.

23. Weiner, S. J.; Kollman, P. A.; Nguyen, N. T.; Case, D. A. *J. Comput. Chem.* **1987**, *7*, 230.

24. Lipton, M.; Still, W. C. *J. Comput. Chem.* **1988**, *9*, 343.

25. Dewar, M. J. S.; Zoebisch, E. G.; Healy, E. F.; Stuart, J. J. P. *J. Am. Chem. Soc.* **1985**, *107*, 3902.

26. TRIPOS, Inc.: St Louis, Missouri, 1994.

27. Farrar, J. R.; Hoss, W.; Herndon, R. M.; Kuzmiak, M. *J. Neurosci.* **1985**, *5*, 1083.

28. Brown, E.; Kendall, D. A.; Nahorski, S. R. *J. Neurochem.* **1984**, *42*, 1379.

29. Periyasamy, S.; Hoss, W. *Life Sci.* **1990**, *47*, 219.

30. Hoss, W.; Woodruff, J. M.; Ellerbrock, B. R.; Periyasamy, S.; Ghodsi-Hovsepian, S.; Stibbe, J.; Bohnett, M.; Messer, Jr W. S. *Brain Res.* **1990**, *533*, 232.

31. Glowinski, J.; Iversen, L. L. *J. Neurochem.* **1966**, *13*, 655.

32. Wreggett, K. A.; Irvine, R. F. *Biochem. J.* **1987**, *245*, 655.

33. Periyasamy, S.; Liu, Y.; Dunbar, P. G.; Rho, T.; Abuh, Y. F.; Messer, Jr W. S. In *Society for Neuroscience*; Society for Neuroscience: Washington, DC, 1993; p 460.

(*Received in U.S.A.* 22 *January* 1996; *accepted* 20 *May* 1996)